Proc. Natl. Acad. Sci. USA
Vol. 83, pp. 6179–6183, August 1986
Neurobiology

Digital imaging of free calcium changes and of spatial gradients in growing processes in single, mammalian central nervous system cells

(growth cones/Ca^{2+}/fluorescent indicators)

JOHN A. CONNOR

AT&T Bell Laboratories, Murray Hill, NJ 07974

Communicated by John J. Hopfield, May 5, 1986

ABSTRACT **Intracellular free calcium levels have been measured in cultured central nervous system (CNS) cells by using the fluorescent indicator fura-2 and digital imaging techniques. Cells were plated from rat embryo diencephalon (embryonic day 17 or 18), with nearly all of the cells surviving dissociation having undergone final mitosis within the previous 24 hr. The initially spherical cells were observed within the first 24 hr in culture when they were extending processes but had not established a network of fibers that would prevent the identification of the origin of a given fiber. Cells that were rapidly extending showed high Ca^{2+} levels in the regions of growth. Where processes had just emerged from the soma or where growth was proceeding from more than one pole, Ca^{2+} levels were uniform and estimated levels of 500 nM were commonly seen. In active growth cones distant from the soma, Ca^{2+} levels exceeded 200 nM, whereas the soma levels were in the 60–80 nM range. Nonextended and extended cells that had stalled had uniform Ca^{2+} levels in the range of 30–70 nM. The results show that high Ca^{2+} levels are at least a correlate of extension in CNS cells and that under some conditions the region of high calcium can be localized to a small part of the cell.**

An understanding of the dynamics of outgrowth in cells of the mammalian central nervous system (CNS) is a critical prerequisite to understanding cell recognition and pattern formation within the CNS. Among the factors that may control outgrowth in developing neurons and other cells is the internal free calcium level in extending regions (growth cones). Elevated calcium levels, by analogy to other motile and secretory systems, could allow the local activation of actinomyosin systems to stretch or shape a growing region or promote the insertion of new membrane, as in vesicular secretion, and thereby produce outgrowth. Recent electrophysiological data indicate that transmembrane Ca transport activity exists in growth cones (1–6), suggesting the possibility of elevated Ca^{2+} concentration. The present study has employed fluorescent Ca indicators (7–10) and a cooled, charge-coupled device (CCD) camera of the type used in astronomy over the past several years (11, 12) to image free Ca^{2+} levels in individual cultured CNS cells from rat embryo. Such combinations have made it possible to follow short-term changes in the spatial distribution of Ca^{2+} during physiological events in single cells (13–17). It is shown that cells undergoing rapid extension display very high internal Ca^{2+} levels and that, where growing processes have extended a significant distance from the soma, the high level is localized to the growing tips. Cells in which growth has been arrested show low internal Ca^{2+} that is uniform throughout the cell.

The publication costs of this article were defrayed in part by page charge payment. This article must therefore be hereby marked "*advertisement*" in accordance with 18 U.S.C. §1734 solely to indicate this fact.

METHODS

Cells from embryonic rat (embryonic day 17 or 18) diencephalon were trypsin-dispersed, plated on no. 1 glass coverslips coated with poly(D-lysine) at 2×10^3 cells per mm^2, and maintained in serum-free defined medium as described elsewhere (18). Fura-2/AM (Molecular Probes, Junction City, OR) was dissolved in dimethyl sulfoxide at 5 mg/ml to make a stock solution. Loading solutions were made by adding the stock to the serum-free defined medium to give nominal concentrations of 4–6 μM. Cells were bathed in the loading solution for 25–30 min at 36°C, allowing the permeant form of the indicator to enter the cells, then rinsed, and given a 1.5- to 3-hr postincubation in defined medium to allow deesterification of the indicator (9, 19).

Plated cells were mounted in a temperature-controlled chamber (33–36°C) containing either Krebs saline or defined medium that allowed direct access to the coverslip underside and placed on the stage of a Zeiss IM-35 microscope. A Nikon UV-F 40X glycerine immersion objective was used for epifluorescence measurements together with a 100-W Hg lamp (Osram) mounted in the Zeiss housing. The CCD camera (Photometrics, Tucson, AZ, model 81-A) employed an RCA SID 53612 chip, 320×512 pixels. Exposure times of 0.2–0.5 s were employed, depending upon the size of cell, dye loading, and contrast desired. Apparent bleaching of fura-2 was <5% for 20-s exposures to 340-nm excitation at the intensity used in experiments. Excitation wavelengths at 340, 360, and 380 nm were obtained using interference filters (Melles-Griot, 10-nm 1/2 B.W.). Exposure times were controlled by a Uniblitz shutter mounted between the filters and the lamp condenser lens. A neutral density (1.5 OD) filter was used in conjunction with the 360- and 380-nm filters to obtain approximately equal fluorescence image intensity for the two excitation wavelengths. The emission spectrum of fura-2 is centered at 500 nm, and after numerous studies employing an interference filter (500 nm, 50-nm bandwidth) in the light exit path, most experiments were conducted with a 480-nm long-pass exit filter to maximize light transmission. Paired exposures were separated by ≈1.5 s, the time required to change excitation filters. Each frame was corrected for camera dark current and background fluorescence by subtracting a frame of the same excitation wavelength made using a blank coverslip covered to an appropriate depth with the same medium that bathed the cells. Blanks were made each experimental day. Measurements have for the most part employed 340- and 380-nm excitation (nominal, see below), the maximally sensitive wavelengths on either side of the 360-nm crossover point. The formation of *ratio images* should, in principle, normalize for the effects of preparation

Abbreviations: CNS, central nervous system; CCD, charge-coupled device; DIC, differential interference-contrast.

geometry, scattering, and illumination nonuniformity (see ref. 7 and below).

In forming ratios of the data arrays, noncellular areas present a problem in that the representations of light levels are small numbers and are therefore subject to large *relative* variation due to noise. For display purposes, a threshold is declared for the denominator field, and for pixel values below this, the ratio is replaced by a common, arbitrary value corresponding to a color or gray level. For color displays, black has been chosen (Figs. 1 and 3) and an intermediate shade of gray in Fig. 2*B*.

For standardizations of fluorescence ratios and to set bounds on trapped dye concentration, glass coverslips (no. 1) with channels 2.7 ± 0.2 μm deep and 50 μm wide were prepared by chemical vapor etching. One of these coverslips clamped against a plain no. 1 coverslip (etched plate on top, channels inward) gave a cuvette with light path of 4–7 μm, depending on how closely the unetched glass surfaces could be apposed. Actual depth for a given run was calculated from the known channel depth and the two fluorescence values of the filling solution at channel and nonchannel areas. Temperature was controlled by heating a pool of water on the top surface to 38°C. Approximate cell thicknesses were determined by carefully focusing up and down with Nomarski optics at 400× magnification. Newly plated cells (<24 hr in culture) were generally between 5 and 8 μm thick at the soma. A test medium to which fura-2 and calcium buffers were added of the following composition was used: KCl, 110 mM; NaCl, 20 mM; $MgCl_2$, 1.2 mM; 4-morpholinepropanesulfonic acid (Mops) buffer, 10 mM (pH = 7.10). Fluorescence (360-nm excitation) of indicator-loaded cells was compared with that of the cuvette channels filled with fura-2 at known concentrations. Concentrations were in the range of 100–300 μM for newly plated cells. I have observed over the course of loading several different types of cells, and ages in culture, that the ultimate amount of dye trapped does not depend simply on the loading solution concentration and exposure time.

Calcium stocks were prepared by using either EGTA or bis[*o*-aminophenoxy]ethane-*N*,*N*,*N*′,*N*′-tetraacetate (BAPTA) (Molecular Probes) as calcium buffer. Indicator constants for the equation below (see ref. 7) were determined on the microscope in four separate runs.

$$[\mathrm{Ca}] = K_D \left[\frac{R - R_{min}}{R_{max} - R}\right] (F_0/F_s). \quad [1]$$

Minimum fluorescence ratios ($R_{min} = F_{340}/F_{380}$) were between 0.39 and 0.42 for test solutions with no added Ca and 5 mM EGTA or BAPTA. Maximum ratios (R_{max}) were between 9 and 10 for saturating levels of Ca. The ratio of fluorescence at 380-nm excitation at the limiting low and high Ca levels (F_0/F_s) was ≈7.5. Intermediate ratios were measured by using EGTA- or BAPTA-buffered test medium. EGTA or BAPTA concentrations were between 5 and 8.3 mM, with fura-2 concentration at 150 μM, making it a minor buffering component in the mix. Three sets of buffered Ca solutions were checked with an ion-sensitive electrode (Simon Levy, Boston University) to control for errors in making up the stocks. Conversions of ratios to $[Ca^{2+}]$ in the text were made by using Eq. 1 with $R_{min} = 0.4$, $R_{max} = 9.5$, $F_0/F_s = 7.5$, and $K_D = 225$. The total dynamic range of the indicator, in cuvette, in the present instrument, R_{max}/R_{min}, is ≈20, considerably less than the value measured in a standard spectrofluorimeter (see also ref. 7). This difference should arise from a shift of the nominal 340-nm and 380-nm bands toward the powerful 366-nm Hg line in the microscope apparatus.

In the diencephalon cells, cerebellar granule neurons (P. E. Hockberger and J.A.C., unpublished data), and adre-

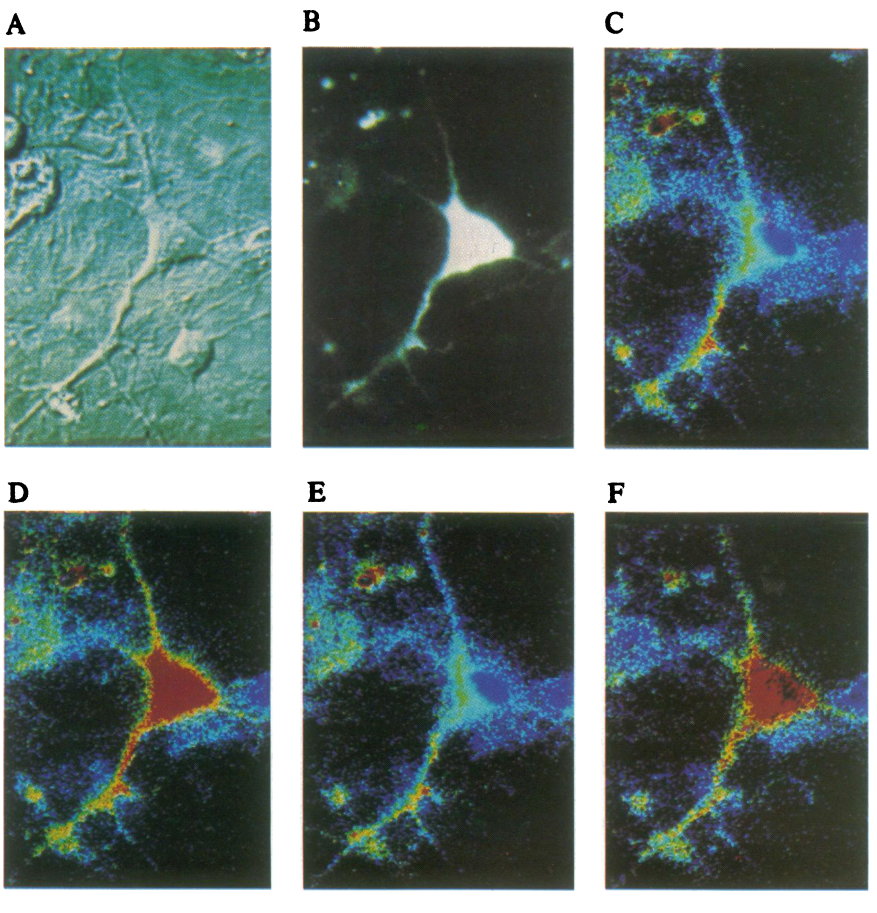

FIG. 1. (*A*) DIC (Normarski) image of bipolar neuron grown 26 days in culture. A small round cell (lower right) failed to trap indicator. (*B*) Fluorescence of trapped indicator (340-nm excitation), illustrating relative intensities in various regions of the cell. The upper process could not be displayed without severely distorting the relative brightness of soma. (*C*) Fluorescence ratio (340/380 nm) of cell bathed in Krebs saline (4.7 mM K). "Haloing" is due to out-of-focus fluorescence and is most severe at the soma, where the cell is thickest. (*D*) Fluorescence ratio of cell exposed to high K saline (25 mM) for 30 s. Red shifted false color indicates higher Ca. Extreme levels of blue and red correspond to ratios of 0.4 and 2.0. (*E*) Ratio 10 min after return to normal saline. (*F*) Ratio image after movement of patch electrode on soma that caused a transient high rate of firing. Dark pixels in the soma are off scale (ratio > 2). (Calibration bar = 10 μm.)

nal glomerulosa cells (J.A.C., C. Cornwall, and G. Williams, unpublished data), the minimum fluorescence ratios (R_{min}) observed were 0.6–0.65. Maximum ratios, R_{max}, observed in response to elevated potassium or the calcium channel agonist leptinotarsin (20) were 5–6. The problem of anomalously low ratio values in unstimulated cells as reported by Almers and Neher (ref. 21; *Methods*) in mast cells was never encountered.

The channel cuvette arrangement also provided a test pattern to check the effectiveness of ratioing in rejecting pathlength and excitation nonuniformities. For example, in an image encompassing channel and nonchannel areas (indicator and Ca concentration uniform), where the blank corrected fluorescence levels were different by a factor of 2, the ratio varied by <1.5%.

RESULTS

Because the imaging method is rather new, a large number of experiments were performed to investigate the behavior of indicator and apparatus under conditions that should give intracellular Ca^{2+} changes. It is well known that in most central neurons, depolarization brings about Ca^{2+} entry (22). When the depolarization is sufficient to trigger action potentials, the Ca influx is greater. In the neural network that exists on the culture plate after several days *in vitro*, elevating potassium in the bathing medium from 4.7 mM to 25 mM is sufficient to cause intense neuron firing.

Fig. 1*A* shows a differential interference-contrast (DIC) picture of a large bipolar neuron grown in culture for 26 days. An extracellular patch recording electrode was sealed onto the soma membrane during the experiment, allowing action potentials and at least a fraction of incoming synaptic input to be monitored. The cell shown was receiving measurable excitatory synaptic input at a mean rate of ≈5 Hz. Most inputs were subthreshold and the cell fired action potentials irregularly at a mean rate of <0.5 Hz in normal Krebs saline.

Fig. 1*B* shows the fluorescence image of this neuron using 340-nm excitation. Fig. 1*C* shows the fluorescence ratio when the cell is in normal Krebs saline. Ratio values have been coded in false color, with increasing values of the ratio shifting from blue to red. It will be noted that the nuclear region of the soma showed the smallest ratio in the resting state (0.65, corresponding to 60 nM), whereas the nonnuclear regions were higher, ≈0.9 (110 nM). Such nonuniformities between nuclear region and other parts of the cell were the rule rather than the exception in hundreds of cells examined. At this point it is unclear whether the difference in ratio reflects a true difference in free calcium or modified dye characteristics in the nucleus. Others (17), having measured *higher* ratios in nuclei of smooth muscle cells, have concluded that the ratio differences reflect true differences in free calcium. At the time of recording, the cell was receiving excitatory input as described above and the region of high Ca^{2+} in the lower neurite may possibly be an input site. Exposing the culture plate to high potassium Krebs saline (25 mM) caused high-frequency action potential firing (≈10 Hz) and a sharp increase in the ratio (Fig. 1*D*) that continued for the duration of the high K exposure (2 min). By using the conversion formula given in *Methods*, the soma ratio predicts a Ca^{2+} level of ≈300 nM during the K exposure, up from the 100 nM levels of nonnuclear cytoplasm in Fig. 1*C*. The increase was not uniform throughout the cell, the proximal neurites showing a smaller increase than the soma. Graubard and Ross (23) have also noted smaller axonal signals from Ca indicator arsenazo III in crustacean neurons during depolarization. A small portion of the soma–neurite difference noted in the present experiment, however, is artifact arising from the relatively faint fluorescence of flat glial cells in the vicinity of, and presumably also underneath, the neuron. This background is usually <5% of the soma fluorescence and 10–15% at the proximal neurites because of the different thicknesses of the structures. The glial signal was relatively insensitive to high K and therefore exists as a constant term in numerator and denominator of a ratio. The ratio values for a more dimly fluorescent region will then be closer to unity than will a bright one. This background is not a problem in very young cultures in which cells have not overgrown the coverslip, but these cells are poorly excitable (24). Reexposing the plate to normal Krebs saline led to a complete

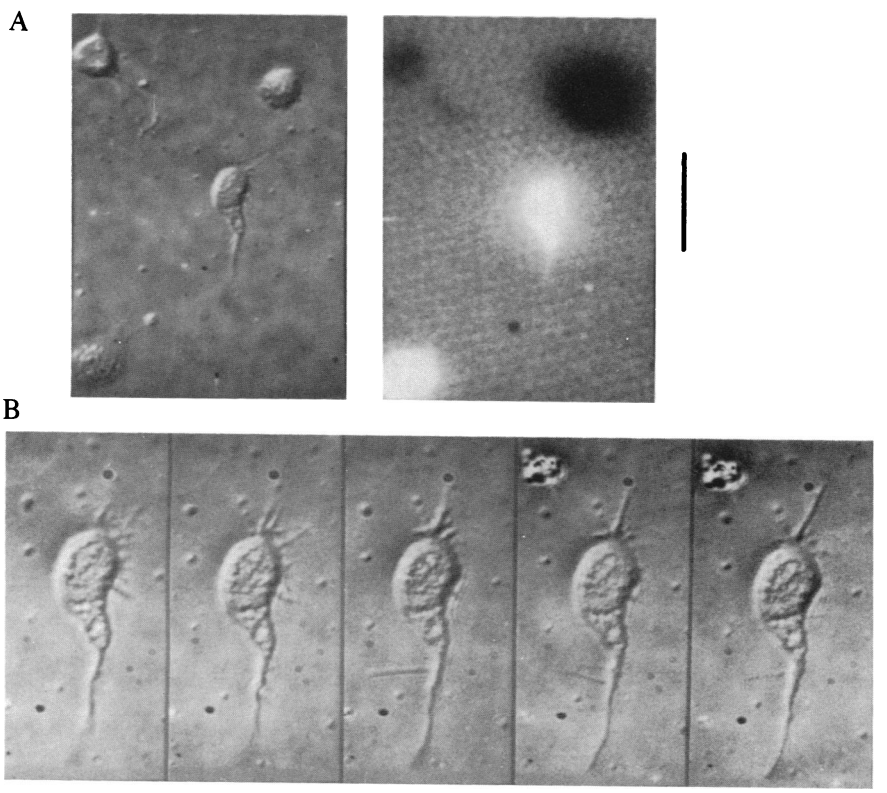

FIG. 2. (*A*) (*Left*) DIC image of a field of four cells plated 16 hr previously. (*Right*) Gray scale ratio image, 340/380, of same field. Ratio values are given in text. The cell in upper right is oversized in the ratio image because of its relative thickness (out-of-focus light) and the necessity of emphasizing contrast at around unity, which was done to keep upper left cell from disappearing into the background. The ratio values in the halo are approximately the same as from the center of the cell. Background gray level was arbitrarily chosen for maximum visibility of cells. (*B*) Enlarged DIC images of center cell taken at ≈4-min intervals illustrating growth rate of high Ca cells. (Calibration bar = 20 μm in *A* and 10 μm in *B*.)

recovery of the initial ratio levels within 1.5 min. Fig. 1*E* shows the ratio 10 min later and illustrates this recovery and the reproducibility generally encountered in experiments. The record of Fig. 1*F* was made just after the patch recording electrode was pushed against the soma. The extracellular electrode monitored high-frequency action potential discharge probably indicative of mechanical pressure upon the cell. The fluorescence ratio became correspondingly larger (predicted $Ca^{2+} > 600$ nM). In other experiments in which tetrodotoxin (0.3 μM) was used to block spontaneous spike activity, a decrease in the fluorescence ratio was noted. The Ca channel blocker nifedipine also caused a decrease in the ratio in a subpopulation of the cells examined.

Growing cell processes were studied in cells no more than 24 hr old that had been plated at approximately one-third the normal density, facilitating the identification of cell processes with their appropriate cell bodies. Coverslips with cells were transferred from the incubator to the microscope stage and equilibrated for 10–15 min in slowly flowing culture medium at 34–36°C equilibrated with a 90% air/10% CO_2 mixture. The coverslip was then scanned for cells or groups of cells that were extending processes. After examining several hundred cell tips, by direct inspection and by time-lapse imaging, it became possible to discriminate between processes that were extending and those that had stalled with a reasonably short inspection. The extension rate of filopodia was generally <0.7 μm/min in the recording chamber and uninterrupted activity was seldom seen for >15 min. The intermittent nature of activity was possibly a result of the perfusion system, which may have dissipated unidentified trophic agents in the medium. Extending processes were often bent toward the direction of flow.

Fig. 2*A* shows a field of four cells as a DIC image (*Left*) and a fluorescence ratio image (*Right*) and illustrates several features usually seen in cultures of this age (20 hr or younger). In the ratio image, displayed on a gray scale, two of the cells are very bright (high Ca), one is about neutral, and one is very dark (low Ca). The three cells on the left had sent out processes, whereas the fourth (upper right) remained rounded as when plated. The two lower cells were in an active growing stage at the time of observation, whereas the upper left cell had essentially stalled. The fluorescence ratios (and corresponding estimates of Ca^{2+}) of the different cells varied from 0.65 (50 nM) in the upper right cell to 3.6 ($\approx$1 μM) in the lower left cell. The centrally located cell showed a ratio of 2.3 (440 nM) in the soma with <20% variation in the processes sprouting from it. The ratio in the soma of the upper right cell was 1.1 (140 nM) with the process about 30% larger, although this difference does not show up at the display scale used here. After the records of Fig. 2*A* were made, the central cell was examined at higher magnification for an extended period (pixel binning in the camera was discontinued giving a 2× enlargement). Fig. 2*B* shows a series of DIC images of this cell taken at 4-min intervals. It is clear that the cell is growing out at both ends, top and bottom, and sprouting side processes as well. Fluorescence images interspersed with these frames showed that the ratio remained around 2 for the duration of the observation period.

High free calcium levels as seen in the lower two cells of Fig. 2*A* do not represent an incompetence in the calcium regulatory system of the cells. Exposing such cells to a simple Hepes-buffered Krebs saline of identical calcium concentration caused a drop in the fluorescence ratio to levels generally below 0.8 within 5 min. Correlated with this decrease was an immediate arrest of growth and often a retraction or restriction of processes. Restoration of medium reversed these changes in a small percentage of cases.

Fig. 3 illustrates the common observation when an actively extending process had reached some distance from the soma. Fig. 3*A* is a DIC image showing extended filapodia at the tip of an outgrowth. Fig. 3 *B* and *C* show the fluorescence images of the cell with 340- and 380-nm excitation. Fig. 3*D* shows the ratio of the fluorescence images, the free Ca levels in the cell. The ratio in the extreme tip is between 1.45 and 1.65 and in the major portion of the cell body is between 0.65 and 0.75. These ratios correspond approximately to free Ca levels in the tip of 230–270 nM and 50–70 nM in the cell body. It will be noted that there are regions of intermediate and lower levels along the process. During the course of a 25-min observation on this cell, the pattern of extension shifted from one in which only the extreme upper part of the tip was involved to the one shown in the figure in which most of the tip has sprouted filopodia. The region of localized high Ca spread concurrently with this change. Again, substitution of Krebs saline for growth medium caused a rapid drop in the high Ca regions. The free Ca levels of stalled growth cones were within 10% of the cell body whether all filopodia had been retracted or not.

Table 1 presents a summary of the observations categorized according to cell extension activity—rapid, slow, stationary. The rapidly extending category includes cells that were sprouting very near the soma and had rather uniformly high calcium levels and those in which substantial processes had already been put down and extension was occurring at the end of these. In the latter cases (Fig. 3) free calcium was only high at the extending tip and a large intracellular gradient of free calcium existed in the cell. The number of cells scored in the intermediate category, slowly extending, was relatively small primarily because it was impractical to spend the time required to decide that the cell was doing anything at all.

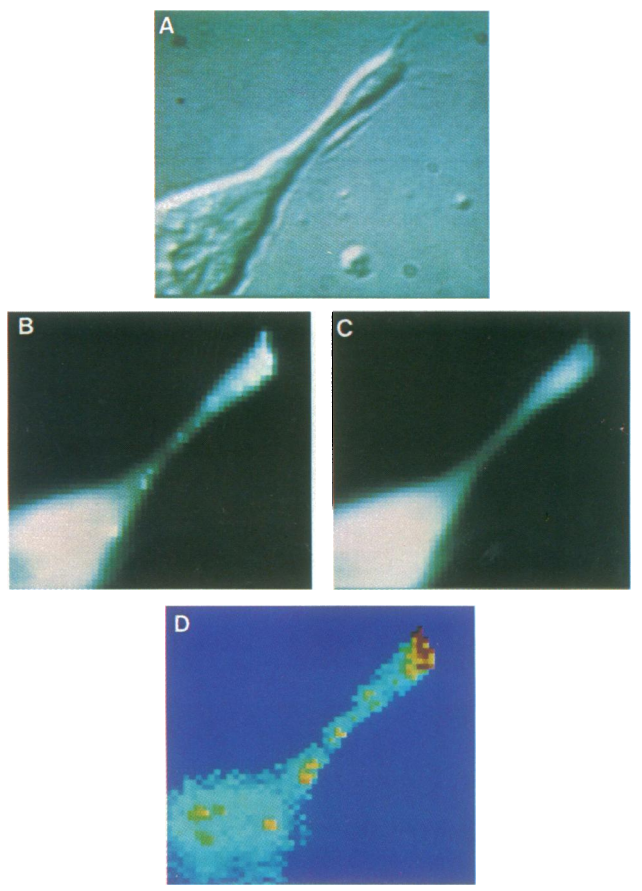

FIG. 3. (*A*) DIC image of cell 20 hr in culture sending out filopodia (upper right). (*B*) Fura-2 fluorescence, 340-nm excitation. (*C*) Fluorescence, 380-nm excitation. (*D*) Ratio of fluorescence images displayed in false color map. The ratio value of color and corresponding calcium level are given in the text. (Calibration bar = 5 μm.)

Table 1. Compilation of data showing correlation of Ca^{2+} levels with extension rate

Cell state	Number observed	Fluorescence ratio at active region	Estimated free Ca^{2+}, nM
Extension at 0.3 μm/min or more	34	1.4–3.5	200–1000
Random movement or slow outgrowth	16	0.8–1.4	70–200
Preextension stage or stalled	>150	0.6–0.8	30–70

Many more cells than the 16 noted were observed at intermediate free calcium levels and the great majority of these cells had growth substantial processes at the time of observation. Stationary cells vastly outnumber the active ones in part because scoring has been done over a population for which the proper growing conditions in the recording chamber were being worked out.

DISCUSSION

The results show a clear correlation between cell growth and high internal free calcium. During stationary periods or when processes were observed to retract, calcium levels were much lower and relatively uniform. In more mature cultures (2–5 days), fluorescence ratios of >0.7–0.9 were almost never observed. At later stages where spontaneous electrical activity was present, the ratio again tended upward in some neurons (as in Fig. 1) but almost never near the 2.0 level unless the cells were stimulated by high K or other means. The observations on growing cells reported are in agreement with studies using electrical techniques in other preparations that have shown a calcium influx into growing tips by means of either Ca spikes (3–5) or a mechanism that carries steady calcium current measurable by external vibrating probe electrodes (2). It was noted in the vibrating probe studies that currents were not generated by stationary growth cones, only those in an active growth state. With the possible exception of cells used in the vibrating probe study, the electrical studies have been carried out on cells that had well-expressed ion channel populations, being either cell lines or regenerating tissue. These diencephalon cells had undergone final mitosis within the 24-hr period preceding isolation and were electrically inexcitable for the first 20 hr after plating (24).

Nifedipine (5 μM), a Ca channel blocker in many nerve cultures, was ineffective in stopping growth or reducing high calcium levels where they were present. Tetrodotoxin was also ineffective. The inorganic Ca channel blockers Cd and Mn disrupted cell growth but had interactions with the intracellular fura-2 (and with quin2) in these and other culture cells that made the experiments uninterpretable (J.A.C. and P. E. Hockberger, unpublished data). Therefore, at present, the mechanism responsible for maintaining the high free calcium levels is not understood. Unlike some amphibian cells (25), these mammalian CNS cells do not sprout processes to any normal degree or even survive well in Ca-free medium (H. Y. Tseng and J.A.C., unpublished data).

The existence over periods of minutes of Ca gradients within a cell such as those observed in Fig. 3 would seem to require the presence of localized Ca influx at the growing tip with efflux or storage predominating over the rest of the cell or else internal compartmentalization as in vesicles or organelles at the growing tip. It is known from other studies that fura-2 does become trapped in intracellular compartments (17, 21) as well as the cytoplasm. Thus, the possibility exists that the locally high Ca in the growing tips is trapped in vesicles too small and densely packed to be resolved, even using a 100× objective as was the case in some experiments. It should be emphasized though that the content of such putative vesicles was very sensitive to the extracellular environment because the gradients were largely abolished within 2–3 min of the withdrawal of medium and its substitution by Krebs saline.

The data shown here have been of fura-2 fluorescence. Earlier experiments (13, 14) used quin2 and showed the same essential features as the fura-2 data with the interesting exception that the regions of high calcium were never so localized, probably the result of higher indicator concentration. These techniques can be effectively applied to study a variety of physiological questions—for example, regional distributions of Ca^{2+} channels or transport into cells, dynamic changes in Ca^{2+} levels in response to neuroactive substances, and development of effective synaptic connections.

Software for the imaging system was written by K. L. McMillan. Thanks is expressed to A. J. Tyson for advice on CCD cameras, to Z. Ahmed, P. E. Hockberger, and H. Y. Tseng for assistance in tissue culture preparations, and to G. Blonder for fabricating calibration slides. Partial support was provided by Air Force Office of Scientific Research Contract F496 20-85-C-0009.

1. Anglister, L., Farber, I. C., Shahar, A. & Grinvald, A. (1982) *Dev. Biol.* **94,** 351–365.
2. Freeman, J. A., Manis, P. B., Snipes, G., Mayes, B., Samson, J., Wikswo, J. & Freeman, D. (1985) *J. Neurosci. Res.* **13,** 257–283.
3. Grinvald, A. & Farber, I. C. (1981) *Science* **212,** 1164–1167.
4. Huttner, S. L. & O'Lague, P. H. (1982) *Soc. Neurosci. Abstr.* **8,** 124.
5. MacVicar, B. A. & Llinas, R. (1982) *Soc. Neurosci. Abstr.* **8,** 914.
6. Spitzer, N. C. (1979) *Annu. Rev. Neurosci.* **2,** 263–297.
7. Grynkiewicz, G., Poenie, M. & Tsien, R. Y. (1985) *J. Biol. Chem.* **260,** 3440–3450.
8. Pozzan, T., Lew, D. P., Wollheim, C. B. & Tsien, R. Y. (1983) *Science* **221,** 1413–1415.
9. Tsien, R. Y., Pozzan, T. & Rink, T. J. (1982) *J. Cell. Biol.* **94,** 325–334.
10. Tsien, R. Y., Rink, T. J. & Poenie, M. (1985) *Cell Calcium* **6,** 145–157.
11. Tyson, A. J., Baum, W. A. & Kreidl, T. (1982) *Astrophys. J.* **252,** L1.
12. Tyson, A. J. & Boeshaar, P. C. (1983) in *Proceedings of the International Astrophysics Union Colloquium,* eds. Philip, A. G. D. & Upgren, A. R. (Davis, Schenectady, NY), p. 85.
13. Connor, J. A. (1985) *Soc. Neurosci. Abstr.* **11,** 176.
14. Connor, J. A. (1985) *Biophys. J.* **47,** 489a (abstr.).
15. Keith, C., Ratan, R., Maxfield, F., Bajer, A. & Shelanski, M. (1985) *Nature (London)* **316,** 848–850.
16. Kruskal, B. A., Keith, C. H. & Maxfield, F. R. (1984) *J. Cell. Biol.* **99,** 1167–1172.
17. Williams, D. A., Fogarty, K. E., Tsien, R. Y. & Fay, F. S. (1985) *Nature (London)* **318,** 558–561.
18. Ahmed, Z., Walker, P. S. & Fellows, R. E. (1983) *J. Neurosci.* **3,** 2448–2462.
19. Tsien, R. Y. (1981) *Nature (London)* **280,** 527–528.
20. Koenig, M. L., Connor, J., Hsaio, T. & McClure, W. O. (1985) *Soc. Neurosci. Abstr.* **11,** 794.
21. Almers, W. & Neher, E. (1985) *FEBS Lett.* **192,** 13–18.
22. Tsien, R. W. (1983) *Annu. Rev. Physiol.* **45,** 341–358.
23. Graubard, K. & Ross, W. N. (1985) *Proc. Natl. Acad. Sci. USA* **82,** 5565–5569.
24. Ahmed, Z., Connor, J. A., Tank, D. & Fellows, R. (1986) *Dev. Br. Res.*, in press.
25. Henderson, H. D., Smith, M. A. & Spitzer, N. C. (1984) *Soc. Neurosci. Abstr.* **10,** 924.